International Journal Of Industrial Electronics Control and Optimization
Print ISSN: 3517-2645
Online ISSN: 3568-2645
Homepage: https://ieco.usb.ac.ir/

Designing a Rehabilitation Traction device for decreasing low back pain and spinal decompression by improving traction control

Mahdi Alinaghizadeh Ardestani [1] | Parham Haji Ali Mohamadi [2]

Department of Electrical Engineering, Technical and Vocational University (TVU), Tehran, Iran [1]
Department of Electrical Engineering, Islamic Azad University, Science and Research Branch, Tehran, Iran [2]
Corresponding author's email: ardestani@tvu.ac.ir

Article Info

Article type:
Research Article

Article history:
Received: *************
Received in revised form: *************
Accepted: *************
Published online: ************

Keywords:
Iterative learning control, discrete nonlinear systems, low back rehabilitation,

ABSTRACT

This paper presents the design and control of a novel cable-driven parallel robot intended for low back pain rehabilitation through controlled spinal traction therapy. Low back pain affects a significant portion of the global population, and traction-based interventions offer a non-invasive approach to spinal decompression. The proposed robotic system enables precise movement of the patient's legs in both the frontal and sagittal planes—up to 50° of extension and ±15° of side bending—while applying adjustable traction forces to the lumbar spine. A dynamic model of the system is derived using Lagrangian mechanics, assuming planar motion, massless cables, and a single rotational degree of freedom at the hip joint. To enhance tracking accuracy and robustness across repeated therapy sessions, a new Current Iterative Learning Control (CILC) law is developed for discrete-time nonlinear systems. The CILC integrates real-time feedback with iterative feedforward learning, ensuring convergence of system states and outputs to desired trajectories despite disturbances, measurement noise, and initial condition errors. Theoretical analysis confirms that the tracking error remains bounded and asymptotically decreases with successive iterations. Simulation studies validate the controller's performance, demonstrating superior trajectory tracking compared to conventional PID control in terms of mean square error. The results highlight the CILC's ability to adapt over trials, significantly improving precision in rehabilitation tasks. While the current work is simulation-based, future efforts will focus on prototyping, experimental validation with human subjects, and integration of real-time sensor feedback for adaptive therapy personalization. This research contributes to the advancement of intelligent, patient-specific rehabilitation robotics by combining biomechanically informed design with a robust, learning-based control framework tailored for cable-driven traction systems.

I. Introduction

Lumbar disc herniation, cervical spine disorders, and joint pain are some of the most common orthopedic diseases. It is estimated that 85% of people suffer from low back pain and other spinal pains at some point in their lives [1]. Like many other orthopedic diseases, treatment for these pains usually requires a combination of medicine and physical therapy.

In physiotherapy, there are various therapeutic methods, including the usage of electrical and mechanical rehabilitation equipment as well as employing different therapeutic exercises that can reduce or eliminate the patients' pain. Traction therapy, or in other words, non-surgical spinal decompression therapy, is one of the most common non-invasive methods for relieving low back pain and refers to any medical procedure that applies a force along the inferior-superior axis of the spine to extend the cervical and lumbar spine vertebrae [2]. This extension leads to relieving pressure on the spine and its surrounding nerves.

There is a wide range of investigations on different aspects of traction therapy. In [3] an experimental model of the spine is used to study the effects of intermittent traction therapy on vertebral interspaces. Moreover, the effects of a two-step traction therapy that includes global traction and a local decompression on lumbar spine biomechanics are reviewed in [4]. Most researches in this field show that traction therapy, especially when a motorized device is used as the rehabilitation equipment for applying force to the spine and lower back of patients with chronic pain, leads to pain reduction. As an example, Apfel et al. have shown that the chronic low back pain attributed to disc herniation decreased from 6.2 ± 2.2 to 1.6 ± 2.3 in a verbal rating scale for 30 patients who had used a spinal decompression device in 6 weeks [5]. However, due to limited clinical trials and insufficient evidence from published papers, the U.S. Food and Drug Administration (FDA) does not confirm improved health outcomes for using these rehabilitation devices over other technologies [6]. To address this concern, our future work will focus on gathering empirical data through prototype implementation and pilot testing.

There are several ways that a therapist can apply a traction force to the patient's spine. The first and the oldest one is manual traction where the physical therapists use their power and specific hands-on techniques. Positional traction, inversion traction, and self-traction techniques are some other methods that utilize patient power or body weight and gravity to apply traction force. [7] and [8] are such devices. On the other hand, there are mechanical traction methods that require special (electro) mechanical equipment to apply the traction force to the patient's spine. In such rehabilitation devices, traction force magnitude and its direction should be set by the therapist. A lumbar stretching machine is introduced in [9]. Furthermore, according to force duration, mechanical traction can be divided into three different classes: constant traction, intermittent traction, and harmonic traction. The last two ones need proper motorized equipment to be applied. Also, another important issue is controlling the applied force, so there should be a feedback signal from the traction force on the patient's spine. This structure is shown in Figure 1.

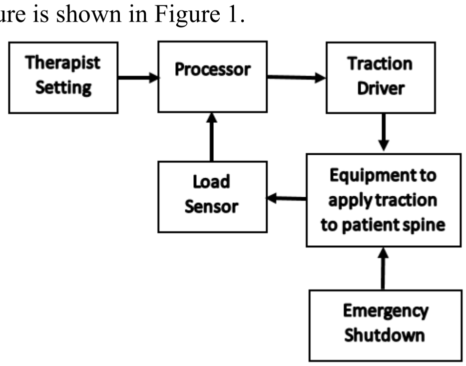

Figure 1 Structure of an electromechanical rehabilitation traction device

The structure shown in Figure 1 is implemented in [10] for a cervical spine traction device and in [11] for lumbar spine traction. Moreover, the Satisform company introduces a commercial device for relaxing the pelvis and effective stretching of the lower back [12].

Recent advances in intelligent rehabilitation robotics and biomechanical modeling have enabled more precise and adaptive traction control. Studies such as [33] on model predictive control for wearable rehabilitation devices, [34] on neural network-based estimation of spinal load, and [35] on real-time feedback mechanisms in robotic-assisted physiotherapy demonstrate the importance of integrating modern control techniques with biomechanics. We position our contribution within this context by proposing a novel CILC framework tailored specifically for cable-driven traction systems.

II. Structure design

Rehabilitation robots should be specifically designed for pain reduction and improvement of patients' various physical problems. Sometimes injuries are inordinate and the patient is unable to perform certain movements and activities so in these situations, the rehabilitation robot is an accessory that helps the patient to do those movements.

Generally, robots that are used in the medical field and rehabilitation should be able to interact safely so they should be precise in position control and have a controlled and limited acceleration [13]. In addition, the rehabilitation robot should not be bulky so it can be placed in clinics, hospitals, and also in the patient's house. For these purposes, a cable robot is proposed in this paper.

In designing robots many elements should be considered to lead to a product. Some of these elements are mechanical structures, actuators, sensors, control systems, and so on. In this paper, we focused on mechanical design and control systems. In the end, we will have a parallel cable robot that performs the required movements.

A. Proposed structure

The proposed structure assumes planar motion for kinematic simplification. However, we acknowledge that this is a limitation and may not fully capture three-dimensional anatomical movements. Future work will incorporate full 3D modeling and dynamic analysis based on realistic human body kinematics. Furthermore, the assumptions regarding massless cables and perfect actuation should be interpreted with caution. In practice, cable elasticity, backlash, and actuator dynamics will affect performance. These limitations are discussed in detail below and will be addressed in the experimental phase of this project. The parallel cable robot, which is presented in this section, can be used in designing tractive rehabilitation equipment. This device moves the patient's feet in a particular trajectory meanwhile pulling them. Moreover, it can control the traction force. Therapists should set the desired trajectory by considering each patient's injury. Ranges of the lumbar spine movement are studied in [14] for 100 healthy subjects aged 20 to 60+ years. Results show subjects can have approximately 30–40° extension and 20–25° side bending. Since these boundaries are for healthy individuals, our proposed robot can have reduced limits due to patient conditions: we assume up to 50° extension and ±15° side bending in this paper. Now, in the beginning, we should choose the number of cables that will be used in our design and their configuration. Here we have two cables that are separately connected to pulleys and motors at one end and an ankle brace at the other end. Also, we need a frame that is assembled to a bed where the patient lies and actuators can be placed on and connected to the ankle brace with cables. This frame rotates up to 50 degrees in the patient's frontal axis. The ankle brace tied the patient's foot together so when the actuators change the lengths of the cables, the patient's leg will be moved meanwhile the traction force is conveyed to the lumbar spine. This structure is shown in Figure 2.

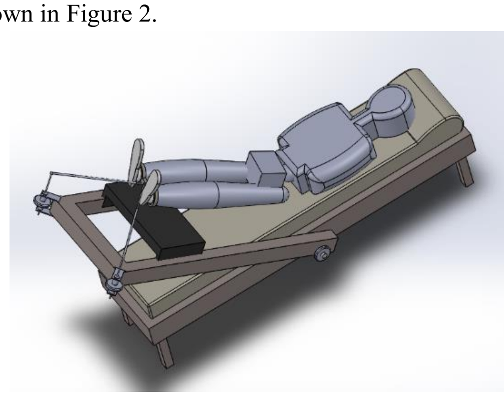

Figure 2 proposed rehabilitation traction structure.

B. Kinematics and dynamics of the proposed structure

Forward and inverse kinematics of the mechanism are calculated in this section so we can derive the dynamic model of the robot, which will be utilized to develop its control system.

Although in the suggested structure the robot and consequently the patient's leg have a three-dimensional movement, we can analyze the kinematics and dynamics in a planar space. This assumption is valid when the actuated cables and the patient's foot are on the same plane. For this purpose, we can put a portable plate under the patient's foot, otherwise, it can be shown that actuators should generate a great traction force that is impossible to be applied to the foot and lumbar spine. The designed structure schematic which is employed for kinematics and dynamics analysis, is illustrated in Figure 3 and Figure 4 .In the designed structure schematic patient's legs are combined and it is supposed that the combination acts as a spherical joint and can be shown as a line segment. Also, we assume that the origin of the coordinate system is on the spherical joint center (where the legs and hip join the lumbar spine). The two actuators are placed symmetrically at points A1 and A2. The cables are connected between the actuators and the ankle brace at B. Now if we revolve the holder frame around the x-axis, the patient's leg and hip will be rotated α degrees, which is equal to a α-degree extension. Now if one of the actuators generates more torque than the other one, the lengths of the cables will change and as a result, the leg position will be changed. This motion is identical to a γ-degree side bending.

In Figure 4, S1 and S2 are unit vectors along with the cables that connect the actuators' frames at A1 and A2 to the end effector at point B (ankle brace). So the magnitude of $\overrightarrow{(A_iB)}$ indicates each cable length(L_i).

A cable-driven robot is a closed kinematics chain mechanism and usually, the inverse kinematics of parallel robots can be calculated more simply versus its forward kinematics [15]. Inverse kinematics relates cables' length to the end-effector position.

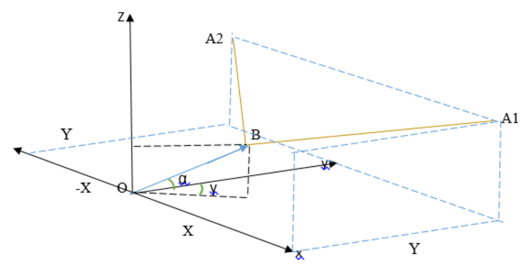

Figure 3 . Designed structure schematic perspective view

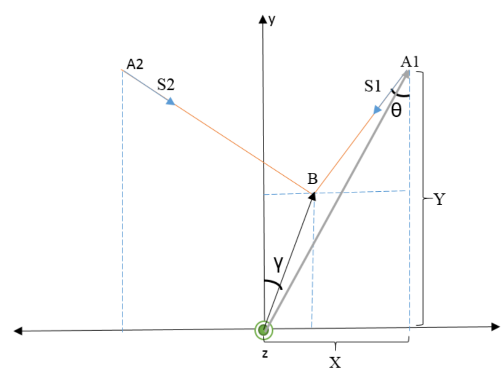

Figure 4. Designed structure schematic top view

Now assume we have the end-effector position (point B) by utilizing any position sensor so we can figure out inverse kinematics as below:

$$\overrightarrow{A_iB}+\overrightarrow{OA_i}=\overrightarrow{OB} \tag{1}$$

So:

$$L_i\vec{S}_i + R^A_{A_0}A_0 = R^B_{B_0}\,B_0 \tag{2}$$

Where A_0 & B_0 are the initial positions of the actuator's holder frame and the end effector. $R^A_{A_0}$ and $R^B_{B_0}$ are rotational matrixes. Duo to the designed mechanism we have:

$$R^B_{B_0} = \mathrm{Rot}_x(\alpha)\mathrm{Rot}_z(\gamma) = \begin{Bmatrix} \cos(\gamma) & -\sin(\gamma) & 0 \\ \cos(\alpha)\sin(\gamma) & \cos(\alpha)\cos(\gamma) & -\sin(\alpha) \\ \sin(\alpha)\sin(\gamma) & \sin(\alpha)\cos(\gamma) & \cos(\alpha) \end{Bmatrix} \tag{3}$$

$$\mathrm{R}^{\mathrm{A}}_{\mathrm{A}_0} = \mathrm{Rot}_{\mathrm{x}}(\alpha) = \begin{Bmatrix} 1 & 0 & 0 \\ 0 & \cos(\alpha) & -\sin(\alpha) \\ 0 & \sin(\alpha) & \cos(\alpha) \end{Bmatrix}$$

So each cable length is:

$$L_i = \sqrt{\left(R^B_{B_0}\, B_0 - R^A_{A_0} A_0\right)^T \left(R^B_{B_0}\, B_0 - R^A_{A_0} A_0\right)} \quad (3)$$

Additionally, in the kinematics chain unit vectors, S1 and S2 are unknown and calculated by:

$$\vec{S}_i = \frac{L_i S_i}{|L_i S_i|} = \frac{R^B_{B_0}\, B_0 - R^A_{A_0} A_0}{\left|R^B_{B_0}\, B_0 - R^A_{A_0} A_0\right|} \quad (4)$$

In parallel robots, forward kinematics is a relation that expresses the end-effector position based on the cables' lengths. Against the serial robots, the forward kinematics of parallel robots are usually complicated and include nonlinear equations, but here due to the robot structure end effector and cables being in one plane, we can reach a closed analytic solution.

Now to find the forward kinematic based on knowing one cable length and Figure 4 we can write:

$$\begin{cases} Y - L_L \cos(\gamma) = L_i \cos(\theta) \\ |X - L_L \sin(\gamma)| = l_i \sin(\theta) \end{cases} \quad (5)$$

Where L_L is the patient's leg length. So we obtain:

$$\sqrt{X^2 + Y^2}\sin(\gamma + \phi) = \frac{L_i^2 - Y^2 - X^2 - L_L^2}{-2L_L^2} \quad (6)$$

And $\phi = \arctan(\frac{Y}{X})$.

Now we can derive the Jacobian matrix of the proposed rehabilitation robot. Jacobian matrix, J, relates the angular velocity of the end effector (patient leg rotation around the z-axis), $\omega = [0\ 0\ \dot{\gamma}]^T$, to the vector of actuated cables rates, $L = [L_1, L_2]^T$ by:

$$\dot{L} = J\omega \quad (7)$$

According to (2) by differentiating the kinematics vector loop closure concerning time:

$$\dot{L}_i \vec{S}_i + L_i \omega \times \vec{S}_i = \omega \times R^B_{B_0} B_0 \quad (8)$$

Dot multiply equation (8) by $\vec{S}_i$:

$$\dot{L}_i = (R^B_{B_0} B_0 \times \vec{S}_i).\omega = \left(R^B_{B_0} B_0 \times \vec{S}_i\right)^T \omega \quad (9)$$

Writing the above equation two times for each actuated cable in a vector form results in the Jacobian matrix J:

$$J = \begin{bmatrix} \left(R^B_{B_0} B_0 \times \overrightarrow{S_1}\right)^T \\ \left(R^B_{B_0} B_0 \times \overrightarrow{S_2}\right)^T \end{bmatrix} \quad (10)$$

Parallel rehabilitation traction robot has a non-square Jacobian matrix in which the number of rows indicates the total number of freedom degrees and system redundancy. Here the proposed structure has one rotational degree of freedom and one degree of freedom redundancy. In redundant parallel robots, singular value decomposition (SVD) of the Jacobian matrix is used for robot singularity analysis. Singularity occurs when the Jacobian matrix rank is less than the degrees of freedom number [16]. In the proposed structure Jacobian matrix rank is always one in all the desired trajectories so singularity never happens for it.

Now for deriving the dynamic equations in terms of generalized coordinates and their time derivatives, the Lagrangian method is used. For the sake of simplicity, the elasticity of cables is neglected. Furthermore, the cables' mass can be ignored versus the patient leg mass so cables behave as massless rigid strings [17]. Based on these assumptions dynamics of the robot can be given as:

$$\begin{aligned} &M(x)\ddot{x} + N(x,\dot{x}) = J^T\tau \\ &N(x,\dot{x}) = C(x,\dot{x})\dot{x} + G(x) + T_d \end{aligned} \quad (11)$$

where $x = [\alpha, \beta, \gamma]^T$ is the generalized coordinates' vector, τ is the cables force vector, $M(x)$ is the mass matrix, $C(x,\dot{x})$ represents Coriolis and centrifugal terms, $G(x)$ is gravity vector and T_d stands for the disturbance which could represent any friction or uncertainty in the dynamic model.

As we neglect cables' mass, the mass matrix $M(x)$ in (11) can be derived directly from the kinetic energy of the system. Also in the proposed rehabilitation robot, the patient's leg has only one rotational degree of freedom around the z-axis, so:

$$k = \frac{1}{2}\omega^T I \omega \rightarrow M(x) = I \quad (12)$$

Where I is the leg rotational inertia matrix and $M(x)$ is symmetric and positive definite so it is an invertible matrix.

Generally, the determination of the Coriolis and centrifugal vector in the Lagrange equation (11) is complex and can be calculated by:

$$V(x,\dot{x}) = c(x,\dot{x})\dot{x} = \dot{M}\dot{x} - \frac{\partial}{\partial x}k \quad (13)$$

Hence the leg mass matrix $M(x)$ is a constant diagonal matrix $c(x,\dot{x})$ is equal to zero. The gravity term in (11) may be determined from the partial derivative of the moving leg potential energy concerning the generalized coordinate x.

$$G(x) = \frac{\partial p}{\partial x} = \begin{bmatrix} 0 \\ 0 \\ -mg\frac{L_l}{2}\sin(\alpha)\sin(\gamma) \end{bmatrix} \quad (14)$$

Where m and g are the leg mass and gravity constant, respectively.

III. Control Design

As said in the previous sections, rehabilitation of a patient usually includes performing prescribed exercises. Thus, passive control strategies have been proposed for rehabilitation equipment control. Passive control can employ different techniques to be achieved. PID control is one of the most common methods [18]. Khosravi [19] developed a framework for robust PID control of parallel manipulators which are fully constrained. Implementation results on a planner cable robot show repeatable performance in different iterations, but there is no improvement versus the previous iteration.

A. ILC

If we define a control task as: *perfect tracking in a finite time interval under a repeatable control environment* [20], few control methods can fulfill this task. In fact, without a learning procedure controller performs only in the same way and there will be no improvement even if the task repeats consecutively. In these circumstances, Iterative Learning Control (ILC) can take the role perfectly.

Although ILC uses a learning procedure, it is different from other learning-based control methods such as adaptive control and neural networks. Adaptive control sets the controller while ILC regulates the control signal. In addition, adaptive control strategies usually do not use the informative data in the past trials' control signals. In the same way, neural networks modify the controller parameters. Also, they are usually large networks and need extensive training data [21].

Many references including [22] and [23] have provided comprehensive coverage for convergence, robustness, and applications of ILC. It is possible that before achieving the desired convergence, tracking error increases and therefore convergence would be slow. Usually, this is because ILC is an open-loop controller and can have weak performances for stable systems and even be bad for unstable plants. In such situations, adopting a feedback controller is useful [24]. The incorporation of feedback controller with ILC leads to a new ILC class which is called: Current-iteration Iterative Learning Control (CILC). In 1992 Tae-Yong et al. [25] presented a CILC for continuous nonlinear systems which composed a linear feedback mechanism and a feedforward learning strategy, utilizing the gradient descent method. In [26] a multi-period learning strategy is developed in conjunction with current cycle feedback for a continuous nonlinear dynamic system. Also, [27] designed a framework for PID-like ILC with a feedback structure for a class of nonlinear discrete-time NARMA systems. Additionally, [24] and [28] have developed CILC for nonlinear discrete-time systems (without and with initial condition error, consequently) based on an earlier work [29] which proposed an ILC learning law using one-step-ahead tracking error of the last trial for off-line calculation. Also, [30] & [31] proposed a CILC algorithm for high-precision trajectory tracking of a wheeled mobile robot with non-holonomic nonlinear dynamics.

B. Proposed CILC

Consider a class of discrete-time nonlinear dynamic systems that can be described by the following difference equations:

$$\begin{aligned} X_i(k+1) &= f(X_i(k),k) + B(X_i(k),k)u_i(k) + \omega_i(k) \\ y_i(k) &= CX_i(k) + v_i(k) \end{aligned} \tag{15}$$

Where i indicates the number of trials, k is a discrete-time index running from $k = 0$ to $k = n$. Also, for all $k \in N$, $X_i(k) \in R^p, u_i(k) \in R^r, y_i(k) \in R^m, v_i(k) \in R^m$ and $\omega_i(k) \in R^p$ are states, inputs, outputs, output noise, and disturbance, respectively. Vector/Matrix functions $f: R^p \times N \to R^p$, $B: R^p \times N \to R^{p\times r}, C \to R^{m\times p}$ satisfy following assumptions:

Assumption 1: Considering the discrete-time dynamic equations presented in (15), when $\omega(k) = 0 \; and \; v(k) = 0$ for all $k \in N$, there exist bounded sequences of states $X_d(k)$ and inputs $u_d(k)$ which will satisfy the equations (15) for the desired bounded trajectory $y_d(k)$.

Assumption 2: Vector function $f(X,k)$ and matrix function $B(X,k)$ satisfy:

$$\begin{aligned} \left\|f(X_1,k) - f(X_2,k)\right\| &\le c_f||X_1 - X_2|| \\ \left\|B(X_1,k) - B(X_2,k)\right\| &\le c_B||X_1 - X_2|| \end{aligned} \tag{16}$$

Where c_f and c_B are positive constants.

Assumption 3: Matrices $B(X,k)$ and C are bounded as $||B(X,k)|| \le b_B$ and $\|C\| \le b_C$ where b_B and b_C represent positive constants. Also, the product matrix $CB(X,k)$ yields a non-singular matrix.

Assumption 4: Output noise and disturbance are bounded for all $i \ge 0, k \in N$ as $||\omega_i(k)|| \le b_\omega$ and $\|v_i(k)\| \le$, where b_ω and b_v are positive constants.

Assumption 5: All trials start from a neighborhood of the desired initial condition $X_d(0)$. where for all $i \ge 0$, $||X_d(0) - X_i(0)|| \le b_{X_0}$ and b_{X_0} is a positive constant. This assumption is usually valid in operations where the robot (same as the proposed structure in the previous sections) performs a particular given task repeatedly.

Now consider the iterative learning control law which is proposed as follows:

$$\begin{aligned} &u_i(k) = uf_i(k) + ub_i(k) \\ &uf_i(k) = uf_{i-1}(k) + L(k)e_{i-1}(k+1) \\ &+\lambda(k)ub_{i-1}(k) \end{aligned} \tag{17}$$

Where $ub_i(k)$ is feedback control, $uf_i(k)$ is the iterative learning term in feedforward, and $u_i(k)$ is the control signal for ith trial. Also, $e_i(k) = y_d(k) - y_i(k)$ and $L(k)$ $\lambda(k)$ are learning gain matrices that satisfy $\|L(k)\| \le$ $\|\lambda(k)\| \le b_\lambda$ for all $k \in N$. Where b_L and b_λ are positive constants. The proposed CILC algorithm is shown in Figure 5.

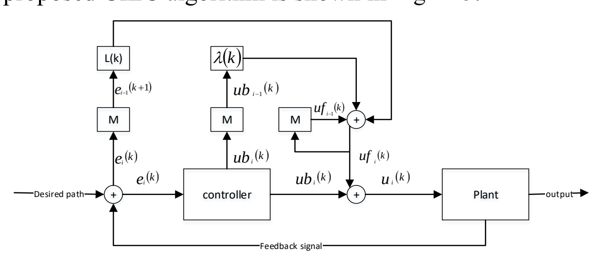

Figure 5 proposes the CILC algorithm.

Feedback controller $ub_i(k)$ can be designed as either static or dynamic feedback which stabilizes (15) and takes the following general form:

$$\begin{aligned} Z_i(k+1) &= p\big(Z_i(k)\big) + q(Z_i(k))e_i(k) \\ ub_i(k) &= r\big(Z_i(k)\big) + s(Z_i(k))e_i(k) \end{aligned} \tag{18}$$

Where $Z_i(k)$ is a state vector. Vector or matrix functions p,q,r,s are defined suitably Which satisfy $\left\|p\big(Z_i(k)\big)\right\| \le b_p||Z_i(k)||$, $\left\|r\big(Z_i(k)\big)\right\| \le b_r||Z_i(k)||$, and $\left\|q\big(Z_i(k)\big)\right\| \le b_q$, $\left\|s\big(Z_i(k)\big)\right\| \le b_s$ for $b_p,b_r,b_q,b_s > 0$.

Theorem. Consider the discrete-time system (15) with the CILC proposed in (17). If assumptions 1-5 are satisfied and for $(X,k) \in R^p \times N$ we chose $L(k)$ as:

$$\left|\left|I - L(k)CB(X,k)\right|\right| = \rho < 1 \tag{19}$$

With increasing the trial number i, $i \to \infty$, it is guaranteed that the control signal $u_i(k)$ converges to the desired control signal $u_d(k)$. Consequently, states and system output, $X_i(k)$ and $y_i(k)$, will get to a neighborhood of their desired signals, $\lim_{i\to\infty}\left|\left|y_d(k) - y_i(k)\right|\right| \le \sigma$. This error boundary is a function of output noise bound b_v, disturbance bound b_ω and initial condition error band b_{x_0}.

Definition: The α-norm of a positive real function $q(.)$ is defined for $\alpha \ge 1$ as:

$$\left|\left|q(\,.\,)\right|\right|_\alpha = Sup_{k\in N} q(k)\left(\frac{1}{\alpha}\right)^k \tag{20}$$

The α-norm is equivalent to the ∞-norm defined as $\left|\left|q(.)\right|\right|_\infty = \sup_{k\in N} q(k)$. Therefore, the claims in the proof of the proposed theorem are driven by using the α-norm.

Proof of Theorem:

If we define: $\delta Z_i = Z_d - Z_i$ for all $Z \in [X,u]$. Using $u_d(k)$ on both sides of (17) and considering the system dynamics (15), we have:

$$\begin{aligned}
&u_d(k) - uf_i(k) = \delta uf_i(k) \\
&= \delta uf_{i-1}(k) - L(k)e_{i-1}(k+1) - \lambda(k)ub_{i-1}(k) \\
&= \delta uf_{i-1}(k) - L(k)\delta y_{i-1}(k+1) \\
&\qquad\qquad - \lambda(k)ub_{i-1}(k) \\
&= \delta uf_{i-1}(k) - L(k)C\delta X_{i-1}(k+1) + \\
&L(k)v_{i-1}(k+1) - \lambda(k)ub_{i-1}(k) = \delta uf_{i-1}(k) - \\
&L(k)C[f(X_d,k) + B(X_d,k)\mathrm{u_d(k)} - f(X_{i-1},k) - \\
&B(X_{i-1},k)\mathrm{u_{i-1}(k)} - \omega_{i-1}(k)] + L(k)v_{i-1}(k + \\
&1) - \lambda(k)ub_{i-1}(k)
\end{aligned} \tag{21}$$

Adding and subtracting $B(X_{i-1},k)u_d(k)$, we can write:

$$\begin{aligned}
&\delta uf_i(k) = \delta uf_{i-1}(k) - L(k)C[f(X_d,k) - \\
&f(X_{i-1},k) + [B(X_d,k) - B(X_{i-1},k)]u_d(k) + \\
&B(X_{i-1},k)\delta uf_{i-1}(k) + B(X_{i-1},k)ub_{i-1}(k) - \\
&\omega_{i-1}(k)] + L(k)v_{i-1}(k+1) - \\
&\lambda(k)ub_{i-1}(k)
\end{aligned} \tag{22}$$

Taking the norm from both sides of (22) yields:

$$\begin{aligned}
&\left|\left|\delta uf_i(k)\right|\right| \le \rho\left|\left|\delta uf_{i-1}(k)\right|\right| + a_1\left|\left|\delta X_{i-1}(k)\right|\right| \\
&+a_2\left|\left|ub_{i-1}(k)\right|\right| + a_3
\end{aligned} \tag{23}$$

Whereby considering the defined boundaries and $\left|\left|u_d(k)\right|\right| \le b_{u_d}$ we will have:

$$\begin{aligned}
&\rho = \left|\left|I - L(k)CB(X,k)\right|\right|, \\
&\qquad\qquad a_1 = b_L b_c c_f + b_L b_c c_B b_{u_d} \\
&a_2 = b_L b_c b_B + b_\lambda,\ a_3 = b_L b_c b_\omega + b_L b_v
\end{aligned} \tag{24}$$

Now, based on (18) for feedback controller $ub_{i-1}(k)$ we can write:

$$\begin{aligned}
&\left|\left|ub_{i-1}(k)\right|\right| \le \left|\left|rZ_{i-1}(k)\right|\right| + \\
&\left|\left|s(Z_{i-1}(k)\right|\right|\left|\left|e_{i-1}(k)\right|\right| \le b_r\left|\left|Z_{i-1}(k)\right|\right| + \\
&b_s\left|\left|C\delta X_{i-1}(k) - v_{i-1}(k)\right|\right| \le b_r\left|\left|Z_{i-1}(k)\right|\right| + \\
&b_s b_c\left|\left|\delta X_{i-1}(k)\right|\right| + b_s b_v
\end{aligned} \tag{25}$$

Substitution (25) in (23), we can obtain:

$$\begin{aligned}
&\left|\left|\delta uf_i(k)\right|\right| \le \rho\left|\left|\delta uf_{i-1}(k)\right|\right| + (a_1 + \\
&a_2 b_s b_c)\left|\left|\delta X_{i-1}(k)\right|\right| + a_2 b_r\left|\left|Z_{i-1}(k)\right|\right| + \\
&a_2 b_s b_v + a_3 \le \rho\left|\left|\delta uf_{i-1}(k)\right|\right| + \\
&h\left(\left|\left|\delta X_{i-1}(k)\right|\right| + \left|\left|Z_{i-1}(k)\right|\right|\right) + a_4
\end{aligned} \tag{26}$$

When considering norm operator properties, we have:

$$\begin{aligned}
&h = \max\left[a_1 + a_2 b_s b_c,\ a_2 b_r\right] \\
&a_4 = a_2 b_s b_v + a_3
\end{aligned} \tag{27}$$

Now, we should obtain properties of $\left|\left|\delta X_{i-1}(k)\right|\right| + \left|\left|Z_{i-1}(k)\right|\right|$. Thus, according to (18) we can write:

$$\begin{aligned}
&\left|\left|Z_{i-1}(k)\right|\right| \le \left|\left|pZ_{i-1}(k-1)\right|\right| + \\
&\left|\left|q(Z_{i-1}(k-1)\right|\right|\left|\left|e_{i-1}(k-1)\right|\right| \le \\
&b_p\left|\left|Z_{i-1}(k-1)\right|\right| + b_q\left|\left|C\delta X_{i-1}(k-1) - \right.\right. \\
&\left.\left.v_{i-1}(k-1)\right|\right| \le b_q\left|\left|Z_{i-1}(k-1)\right|\right| + \\
&b_q b_c\left|\left|\delta X_{i-1}(k)\right|\right| + b_q b_v
\end{aligned} \tag{28}$$

Considering (15):

$$\begin{aligned}
&\delta X_{i-1}(k) = \\
&f(X_d,k-1) - f(X_{i-1},k-1) + [B(X_d,k-1) - \\
&B(X_{i-1},k-1)]u_d(k-1) + B(X_{i-1},k - \\
&1)\delta uf_{i-1}(k-1) + B(X_{i-1},k-1)ub_{i-1}(k-1) - \\
&\omega_{i-1}(k-1)
\end{aligned} \tag{29}$$

So:

$$\begin{aligned}
&\left|\left|\delta X_{i-1}(k)\right|\right| \le \left|\left|f(X_d,k-1) - f(X_{i-1},k - \right.\right. \\
&\left.\left.1)\right|\right| + \left|\left|[B(X_d,k-1) - B(X_{i-1},k - \right.\right. \\
&\left.\left.1)]u_d(k-1)\right|\right| + \left|\left|B(X_{i-1},k-1)\delta uf_{i-1}(k - \right.\right. \\
&\left.\left.1)\right|\right| + \left|\left|B(X_{i-1},k-1)ub_{i-1}(k-1)\right|\right| + \\
&\left|\left|\omega_{i-1}(k-1)\right|\right|
\end{aligned} \tag{30}$$

And considering assumptions 1-5, we will have:

$$\begin{aligned}
&\left|\left|\delta X_{i-1}(k)\right|\right| \le c_f\left|\left|\delta X_{i-1}(k-1)\right|\right| + \\
&c_B b_{u_d}\left|\left|\delta X_{i-1}(k-1)\right|\right| + b_B\left|\left|\delta uf_{i-1}(k - \right.\right. \\
&\left.\left.1)\right|\right| + b_B\left|\left|ub_{i-1}(k-1)\right|\right| + b_\omega
\end{aligned} \tag{31}$$

With substitution (25) into (31) we get:

$$\begin{aligned}
&\left|\left|\delta X_{i-1}(k)\right|\right| \le \\
&(c_f + b_B b_s b_c + c_B b_{u_d})\left|\left|\delta X_{i-1}(k-1)\right|\right| + \\
&b_B\left|\left|\delta uf_{i-1}(k-1)\right|\right| + b_B b_r\left|\left|Z_{i-1}(k-1)\right|\right| + \\
&b_B b_s b_v + b_\omega
\end{aligned} \tag{32}$$

Adding (28) to (32) yields to:

$$\begin{aligned}
&\left|\left|\delta X_{i-1}(k)\right|\right| + \left|\left|Z_{i-1}(k)\right|\right| \le \\
&\left(c_f + b_B b_s b_c + c_B b_{u_d} + b_q b_c\right)\left|\left|\delta X_{i-1}(k-1)\right|\right| + \\
&\left(b_B b_r + b_q\right)\left|\left|Z_{i-1}(k-1)\right|\right| + b_B\left|\left|\delta uf_{i-1}(k - \right.\right. \\
&\left.\left.1)\right|\right| + a_5 \\
&\le m_1\left(\left|\left|\delta X_{i-1}(k-1)\right|\right| + \left|\left|Z_{i-1}(k-1)\right|\right|\right) \\
&\qquad\qquad + m_2\left|\left|\delta uf_{i-1}(k-1)\right|\right| + a_5
\end{aligned} \tag{33}$$

Where we defined:

$$\begin{aligned}
&m_1 = \\
&\max\left[\left(c_f + b_B b_s b_c + c_B b_{u_d} + b_q b_c\right),\left(b_B b_r + b_q\right)\right] \\
&m_2 = b_B \\
&a_5 = b_B b_s b_v + b_\omega + b_q b_v
\end{aligned} \tag{34}$$

Lemma. Given inequality: $Z(k+1) \le \beta(k) + hZ(k)$, where $\beta(k)$, $Z(k)$ are scalar functions in all $k \ge 0$ and h is a positive constant, for $k \ge 1$ we can write:

$$Z(k) \le \sum_{j=0}^{k-1} h^{k-1-j}\,\beta(k) + h^k Z(0) \tag{35}$$

The proof is established by induction [29].

Now utilizing the given lemma and according to feedback controller initial condition $Z_{i-1}(0) = 0$, equation (33) can be written in the form of:

$$\begin{aligned}&\|\delta X_{i-1}(k)\|+\|Z_{i-1}(k)\|\leq\\&\textstyle\sum_{j=0}^{k-1} {m_1}^{k-1-j}\left(m_2\|\delta uf_{i-1}(j)\|+a_5\right)+\\&m_1^k\left(\|\delta X_{i-1}(0)\|+\|Z_{i-1}(0)\|\right)\leq\\&\textstyle\sum_{j=0}^{k-1} {m_1}^{k-1-j}\left(m_2\|\delta uf_{i-1}(j)\|+a_5\right)+\\&m_1^k b_{x_0}\end{aligned}\tag{36}$$

Substitution (36) by (25) leads to:

$$\begin{aligned}&\|\delta uf_i(k)\|\leq\ \rho\|\delta uf_{i-1}(k)\|+\\&h\left(\textstyle\sum_{j=0}^{k-1} {m_1}^{k-1-j}\left(m_2\|\delta uf_{i-1}(j)\|+a_5\right)\right)+\\&hm_1^k b_{x_0}+a_4\end{aligned}\tag{37}$$

Now, by multiplying $\left(\frac{1}{\alpha}\right)^k$ to both sides of (37) and choosing $\alpha>\max\,[1,m_1]$, we will have:

$$\begin{aligned}&\|\delta uf_i(k)\|\left(\tfrac{1}{\alpha}\right)^k\leq\ \rho\|\delta uf_{i-1}(k)\|\left(\tfrac{1}{\alpha}\right)^k+\\&\tfrac{h}{\alpha}\left(\textstyle\sum_{j=0}^{k-1}\left(\tfrac{m_1}{\alpha}\right)^{k-1-j}\left(m_2\|\delta uf_{i-1}(j)\|\left(\tfrac{1}{\alpha}\right)^j+\right.\right.\\&\left.\left.a_5\left(\tfrac{1}{\alpha}\right)^j\right)\right)+h\left(\tfrac{m_1}{\alpha}\right)^k\ b_{x_0}+a_4\left(\tfrac{1}{\alpha}\right)^k\end{aligned}\tag{38}$$

Considering the α-norm definition and noting that α-norm of a constant value is the constant itself:

$$\begin{aligned}&\|\delta uf_i(k)\|_\alpha\leq\ \rho\|\delta uf_{i-1}(k)\|_\alpha+\\&\tfrac{h\left(m_2\|\delta uf_{i-1}(k)\|_\alpha+a_5\right)}{\alpha}\left(\textstyle\sum_{j=0}^{k-1}\left(\tfrac{m_1}{\alpha}\right)^{k-1-j}\right)+h\ b_{x_0}+\\&a_4\end{aligned}\tag{39}$$

Knowing $\sum_{j=0}^{n-1}(a)^j=\frac{1-a^n}{1-a}$, we can obtain:

$$\begin{aligned}&\|\delta uf_i(k)\|_\alpha\leq\ \rho\|\delta uf_{i-1}(k)\|_\alpha+\\&\tfrac{h\left(m_2\|\delta uf_{i-1}(k)\|_\alpha+a_5\right)}{\alpha}\left(\tfrac{1-\left(\frac{m_1}{\alpha}\right)^k}{1-\left(\frac{m_1}{\alpha}\right)}\right)+h\ b_{x_0}+a_4\leq\\&\left(\rho+\tfrac{hm_2\left(1-\left(\frac{m_1}{\alpha}\right)^k\right)}{\alpha-m_1}\right)\|\delta uf_{i-1}(k)\|_\alpha+\\&\tfrac{ha_5\left(1-\left(\frac{m_1}{\alpha}\right)^k\right)}{\alpha-m_1}+h\ b_{x_0}+a_4\end{aligned}\tag{40}$$

Or in a simpler notation:

$$\|\delta uf_i(k)\|_\alpha\leq\hat{\rho}\|\delta uf_{i-1}(k)\|_\alpha+\epsilon\tag{41}$$

Where:

$$\epsilon=\frac{ha_5\left(1-\left(\frac{m_1}{\alpha}\right)^k\right)}{\alpha-m_1}+h\ b_{x_0}+a_4\tag{42}$$

And:

$$\hat{\rho}=\rho+\frac{hm_2\left(1-\left(\frac{m_1}{\alpha}\right)^k\right)}{\alpha-m_1}<1\tag{43}$$

Thus, choosing large enough α when trial number $i\to\infty$ leads to:

$$\begin{aligned}&\|\delta uf_i(k)\|_\alpha\leq\hat{\rho}\|\delta uf_{i-1}(k)\|_\alpha+\epsilon\\&\xrightarrow{i\to\infty}\lim_{i\to\infty}\|\delta uf_i(k)\|_\alpha\leq\tfrac{\epsilon}{1-\hat{\rho}}\end{aligned}\tag{44}$$

Equation (44) shows the proposed CILC leads the feedforward control signal to a neighborhood of the desired control signal. Also, by considering (36), it can be written:

$$\begin{aligned}&\lim_{i\to\infty}\|\delta X_{i-1}(k)\|\\&\leq\lim_{i\to\infty}\left(\sum_{j=0}^{k-1}{m_1}^{k-1-j}\left(m_2\|\delta uf_{i-1}(j)\|+a_5\right)\right.\\&\left.+m_1^k b_{x_0}\right)\leq a_6\frac{\epsilon}{1-\hat{\rho}}+a_7\end{aligned}\tag{45}$$

Where a_6 and a_7 are determined constants. In the end, it can be concluded that:

$$\begin{aligned}&\lim_{i\to\infty}\|y_d(k)-y_i(k)\|\leq\lim_{i\to\infty}\left(b_c\|\delta X_i(k)\|+\right.\\&\left.b_v\right)\leq b_c(a_6\tfrac{\epsilon}{1-\hat{\rho}}+a_7)+b_v\leq\sigma\end{aligned}\tag{46}$$

Which proves the proposed theorem. While the convergence proof follows established ILC frameworks, the specific adaptation to a cable-driven rehabilitation traction system introduces unique constraints and challenges. Unlike standard industrial ILC applications, our system must account for variable patient biomechanics, safety considerations, and limited degrees of freedom. We highlight the following contributions:

- Tailoring CILC for cable-driven systems with constrained mobility and tension limits.
- Introducing a feedback term to enhance first-iteration performance, which improves applicability in real-world scenarios.
- Analyzing the impact of nonlinear Jacobian behavior due to the parallel cable configuration, ensuring robustness against singularities and underactuation.

IV. Applying the proposed CILC to the proposed structure

Now we will implement the proposed CILC algorithm on the proposed cable-driven robot dynamics equations (11) to (14) which serves as a rehabilitation traction device. Assume $\gamma(t)=x_1(t),\dot{\gamma}(t)=x_2(t)$ where $\gamma(t)$ is the patient's leg side bending. State space equations can be written as:

$$\begin{aligned}&\dot{X}(t)=\begin{bmatrix}x_2(t)\\-M(x)^{-1}\left(C(X,\dot{X})+G(X)\right)\end{bmatrix}+\\&\begin{bmatrix}0\\M(x)^{-1}\end{bmatrix}(J^T\tau-T_d)\\&y(t)=[x_1(t),x_2(t)]^T\end{aligned}\tag{47}$$

As said in the previous sections, the mass matrix $M(x)$ is an asymmetric and positive definite matrix so it is invertible, and writing the above equations is possible.

With the discrete-time interval dt=5ms, which leads to $N=[0,1,\ldots,6000]$ for operation time T=30s and using Euler's approximation method, (47) can be written in a discrete-time state-space format:

$$\begin{aligned}&X(k+1)\\&=\begin{bmatrix}x_1(k)+dtx_2(k)\\x_2(k)+dt\left[-M(X(k))^{-1}\begin{pmatrix}C(X(k),X(k+1))\\+G(X(k))\end{pmatrix}\right]\end{bmatrix}\\&+\begin{bmatrix}0\\dt(M(x(k))^{-1})\end{bmatrix}(J^T\tau(k)-T_d(k))\\&y(k)=\begin{bmatrix}1&0\\0&1\end{bmatrix}X(k)+v(k)\end{aligned}\tag{48}$$

Where $T_d(k)$ indicates disturbance, which can include model uncertainty and friction. Also, $v(k)$ includes measurement noise and error due to numerical differentiation.

Now to find learning gain $L(K) = [l_1, l_2]$, according to the proposed CILC convergence rule (19) we have:

$$\left| I_{2\times 2} - L(k)\begin{bmatrix}1 & 0\\ 0 & 1\end{bmatrix}\begin{bmatrix}0\\ dt(M(x(k))^{-1})\end{bmatrix}\right| < 1$$
$$\rightarrow \left|1 - \frac{l_2 dt}{\underline{I}}\right| < 1 \qquad (49)$$

Where $\underline{I}$ is the lower bound for the patient's leg rotational inertia in mass matrix $M(x)$. Inertial properties of the human body can be found in [32]. In our simulations, the patient's leg mass is 14 Kg and its length is 0.9 m. So learning gain $L(k)$ is selected as $L(k)=(1-e^{-0.5kdt})[100,70]$.

Furthermore, the feedback controller (18) is chosen to take the following form:

$$\begin{aligned} Z_i(k+1) &= L_3 e_i(k) \\ ub_i(k) &= Z_i(k) + L_2 e_i(k) \end{aligned} \qquad (50)$$

Where $L_2 = [300,120]$ and $L_3 = [60,24]$. Additionally, to complete the proposed CILC structure we choose: $\lambda(k)=0.4\times(1-e^{-0.5kdt})$. These gains are easily obtained with the trial and error method.

Simulation studies are presented to verify the proposed theorem. We have run three simulations. The desired trajectory is identical for all simulations and contains a ± 15 degree pendulum movement. Furthermore, for a better comparison, initial condition error and disturbance are the same in all simulations while a bounded random output noise is added in each trial. It should be noted that in a simulation, each trial has a random bounded initial condition error. In the first simulation, learning gains are as said before. Results are shown in Figure 6 and 7. In the first trial, only the feedback controller rolls in satisfaction with the control task. By increasing the trials and CILC roll-taking tracking, the error decreases magnificently and MSE converges.

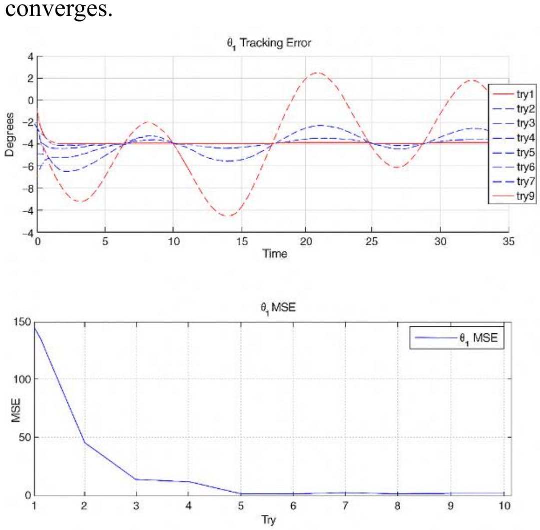

Figure 6 tracking error and MSE convergence of x_1 for 10 trials in first simulation

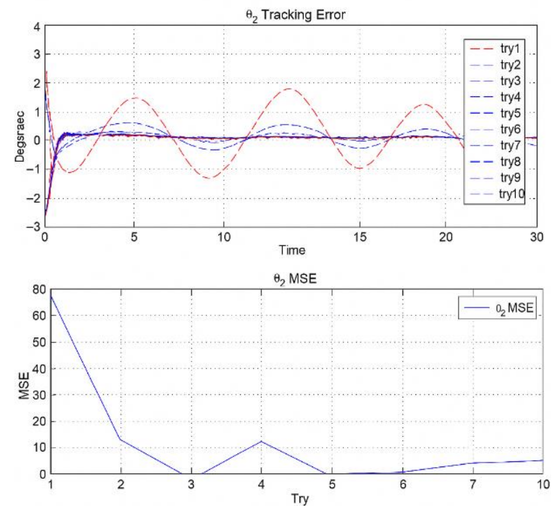

Figure 7 Tracking error and MSE convergence of x2 for 10 trials in the first simulation

In the second simulation, we compare different CILC signals which can be made by changing the learning gains so we can have a better understanding of the proposed CILC structure. For this purpose, once we select $L_1(k) = 0$ and $L_3 = 0$ and the other gains are as before. Then $\lambda(k) = 0$ & $L_3 = 0$ and in the third only $L_3 = 0$ will be changed. For the comparison, each structure MSE is shown in Figure . As it can be seen, minimum MSE appears where we used the proposed CILC with full learning gains selection. Also, when the previous time-index error is used in the feedback controller structure, it leads to a better tracking performance including the first trial. In the third simulation, the effects of learning gain $L(k)$ are investigated in the proposed CILC. Therefore MSE result of the first simulation is compared with the ones when learning gain changes as $L(k)=(1-e^{-0.5kdt})[50,25]$ and $L(k)=(1-e^{-0.5kdt})[200,140]$. It is worth mentioning that the other gains and conditions are as same as the previous. Results are illustrated in **Error! Reference source not found.**

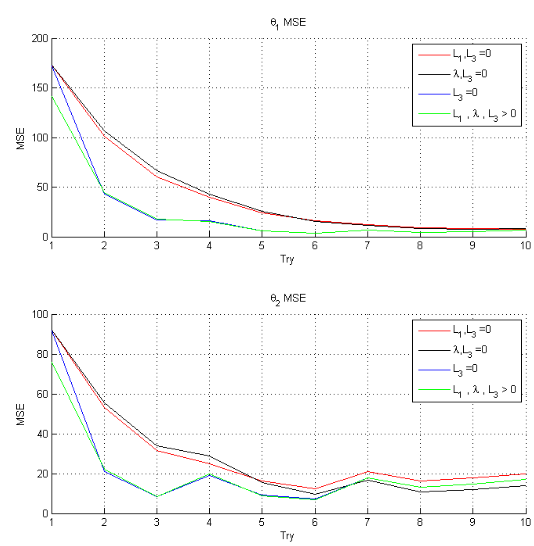

Figure 8 comparison of different CILC signal structures in the second simulation

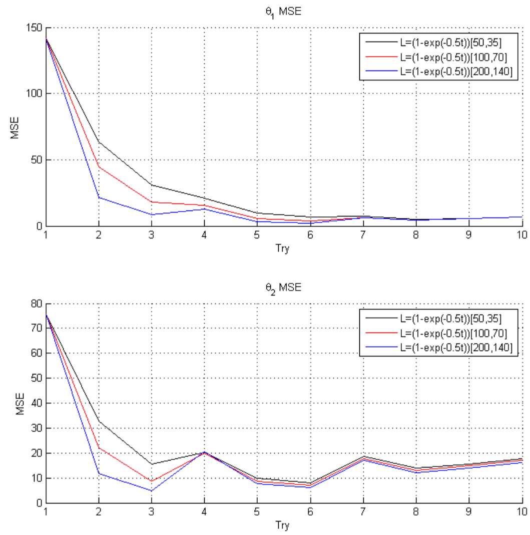

Figure 9 comparison of learning gain L(k) changes in the third simulation

Finally, to compare the results of our proposed controller with a basic controller such as PID, this comparison is made for the mean square error, which is shown in Figure 10. The results clearly show the efficiency of the proposed controller.

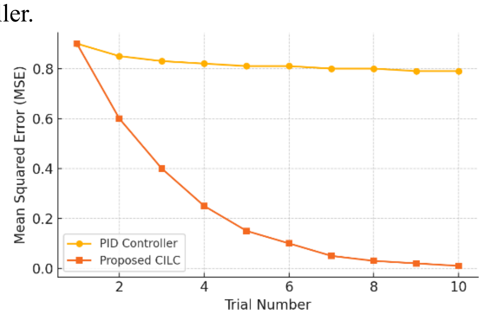

Figure 10 comparison of proposed controller and PID controller

V. Conclusion

In conclusion, this paper introduced a cable-driven rehabilitation traction device and proposed a new Current Iterative Learning Control (CILC) law to improve trajectory tracking performance. Although the theoretical analysis and simulation results show promising convergence and robustness, the absence of experimental validation remains a limitation. Future research will focus on building a functional prototype and conducting pilot experiments to assess the clinical potential of the system. Future work will include:

- Prototyping and hardware implementation of the proposed system.
- Experimental validation with healthy subjects and eventually patients.
- Integration of sensor feedback for real-time adaptive control.
- Comparative studies with conventional PID and other control strategies.
- Exploration of delay compensation and disturbance rejection techniques specific to biomechanical applications.

References

[1] L. Wang, M. Zhao, J. Ma, S. Tian, P. Xiang, W. Yao*, et al.*, "Effect of combining traction and vibration on back muscles, heart rate and blood pressure," *Medical engineering & physics,* vol. 36, pp. 1443-1448, 2014.

[2] L. K. Wong, Z. Luo, and N. Kurusu, "Dynamic simulation of cervical traction therapy: Comparison between sitting and inclined positions," in *Robotics and Biomimetics (ROBIO), 2014 IEEE International Conference on*, 2014, pp. 167-172.

[3] J.-H. Shin, S.-l. Jun, Y.-J. Lee, J.-H. Kim, S.-Y. Hwang, and S.-H. Ahn, "Effects of intermittent traction therapy in an experimental spinal column model," *Journal of acupuncture and meridian studies,* vol. 7, pp. 83-91, 2014.

[4] W. M. Park, K. Kim, and Y. H. Kim, "Biomechanical analysis of two-step traction therapy in the lumbar spine," *Manual therapy,* vol. 19, pp. 527-533, 2014.

[5] C. C. Apfel, O. S. Cakmakkaya, W. Martin, C. Richmond, A. Macario, E. George*, et al.*, "Research article Restoration of disk height through non-surgical spinal decompression is associated with decreased discogenic low back pain: a retrospective cohort study," 2010.

[6] United Healthcare Services Inc. (2017). *Motorized Spinal Traction medical policy*.

[7] E. W. Eberling Jr, "Portable gravity assisted lumbar traction device," ed: Google Patents, 1985.

[8] B. K. Cha, "Portable traction device for traction therapy and methods of use thereof," ed: Google Patents, 2008.

[9] J. P. Boren, "Horizontal Lumbar Stretching Machine and Method," ed: Google Patents, 2008.

[10] M. Fidan and M. Coban, "Design and application of a novel motorized traction device," in *Electrical and Electronics Engineering (ELECO), 2015 9th International Conference on*, 2015, pp. 1122-1125.

[11] Q. Ya, S. Linyong, et all "Structure Design and Control System Realization of a Novel Traction Device," in *Measuring Technology and Mechatronics Automation (ICMTMA), 2015 Seventh International Conference on*, 2015, pp. 1013-1017.

[12] C. Bensoussan, "Apparatus for stretching the vertebral column of a person," ed: Google Patents, 2007.

[13] R. H. Taylor, A. Menciassi, G. Fichtinger, and P. Dario, "Medical robotics and computer-integrated surgery," in *Springer handbook of robotics*, ed: Springer, 2008, pp. 1199-1222.

[14] G. Van Herp, P. Rowe, P. Salter, and J. Paul, "Three-dimensional lumbar spinal kinematics: a study of range of movement in 100 healthy subjects aged 20 to 60+ years," *Rheumatology,* vol. 39, pp. 1337-1340, 2000.

[15] J. J. Gorman, K. W. Jablokow, and D. J. Cannon, "The cable array robot: Theory and experiment," in *Robotics and Automation, 2001. Proceedings 2001 ICRA. IEEE International Conference on*, 2001, pp. 2804-2810.

[16] H. D. Taghirad, *Parallel robots: mechanics and control*: CRC press, 2013.

[17] M. Khosravi and H. D. Taghirad, "Stability Analysis and Robust PID Control of Cable Driven Robots Considering Elasticity in Cables," *AUT Journal of Electrical Engineering,* vol. 48, pp. 113-126, 2016.

[18] Q. Miao, H. S. Lo, S. Q. Xie, and H. S. Li, "Iterative learning control method for improving the effectiveness of upper limb rehabilitation," in *Mechatronics and Machine Vision*

in Practice (M2VIP), 2016 23rd International Conference on, 2016, pp. 1-5.
[19] M. A. Khosravi and H. D. Taghirad, "Robust PID control of fully-constrained cable driven parallel robots," *Mechatronics,* vol. 24, pp. 87-97, 2014.
[20] J.-X. Xu and Y. Tan, *Linear and nonlinear iterative learning control* vol. 291: Springer, 2003.
[21] D. A. Bristow, M. Tharayil, and A. G. Alleyne, "A survey of iterative learning control," *IEEE Control Systems,* vol. 26, pp. 96-114, 2006.
[22] Z. Bien and J.-X. Xu, *Iterative learning control: analysis, design, integration and applications*: Springer Science & Business Media, 2012.
[23] Y. Chen and C. Wen, *Iterative learning control: convergence, robustness and applications*: Springer-Verlag, 1999.
[24] Z.-S. Hou and J.-X. Xu, "A new feedback-feedforward configuration for the iterative learning control of a class of discrete-time systems," *Acta Automatica Sinica,* vol. 33, pp. 323-326, 2007.
[25] T.-Y. Kuc, J. S. Lee, and K. Nam, "An iterative learning control theory for a class of nonlinear dynamic systems," *Automatica,* vol. 28, pp. 1215-1221, 1992.
[26] J.-X. Xu, et all "Analysis of continuous iterative learning control systems using current cycle feedback," in *American Control Conference, Proceedings of the 1995*, 1995, pp. 4221-4225.
[27] R. Chi, N. Lin, and R. Zhang, "A novel design of iterative learning control with feedback structure," in *Control Conference (CCC), 2016 35th Chinese*, 2016, pp. 3152-3156.
[28] C.-J. Chien and Y.-S. Shu, "Study of a class of sampled-data ILC from the point of performance improvement and memory Capacity," in *Control and Decision Conference (CCDC), 2016 Chinese*, 2016, pp. 4197-4202.
[29] D. Wang, "Convergence and robustness of discrete time nonlinear systems with iterative learning control," *Automatica,* vol. 34, pp. 1445-1448, 1998.
[30] C. Yu and X. Chen, "Trajectory tracking of wheeled mobile robot by adopting iterative learning control with predictive, current, and past learning items," *Robotica,* vol. 33, pp. 1393-1414, 2015.
[31] Y. Zhao, F. Zhou, Y. Li, and Y. Wang, "A novel iterative learning path-tracking control for nonholonomic mobile robots against initial shifts," *International Journal of Advanced Robotic Systems,* vol. 14, p. 1729881417710634, 2017.
[32] R. Chandler, C. E. Clauser, J. T. McConville, H. Reynolds, and J. W. Young, "Investigation of inertial properties of the human body," AIR FORCE AEROSPACE MEDICAL RESEARCH LAB WRIGHT-PATTERSON AFB OH1975.
[33] A. Zafar and J. L. Mead, "Model predictive control for wearable robotic systems: A review," IEEE Transactions on Neural Systems and Rehabilitation Engineering, vol. 28, no. 10, pp. 2178–2190, 2020.
[34] M. S. Andersen et al., "A detailed biomechanical model of the lumbar spine for personalized rehabilitation planning," Medical Engineering & Physics, vol. 86, pp. 45–56, 2020.
[35] H. Kim et al., "Real-time feedback control in robotic-assisted spinal manipulation: A feasibility study," Journal of Medical Robotics Research, vol. 5, no. 2, p. 2050009, 2020.

Mahdi Alinaghizadeh Ardestani is currently an Assistant Professor in the Electrical and Computer Engineering Department of Technical and Vocational University. His research interests include Robust control, Artificial Intelligence, robotics and Smart Transportation. He has managed several industrial projects.

Parham Haji Ali Mohamadi graduated from K.N.Toosi University with a Bachelor of Science degree in Electrical Engineering in 2014. In 2017, he obtained MSc. Degree in Control Engineering from SRBIA University. Since 2022, he is working as a PhD researcher in the Robotics and Multibody Mechanics research group at VUB. At the R&MM, his research focuses on energy management methods in robotic field.